Observation of the stochastic realization shift in the weak-field limit

M. P. van Exter, D. M. Boersma, A. K. Jansen van Doorn, and J. P. Woerdman

Huygens Laboratory, University of Leiden, P.O. Box 9504, 2300 RA Leiden, The Netherlands

The amplitude-phase coupling of a stochastically varying field has been predicted to lead to a shift of the effective resonance frequency when this field interacts with a two-level system. Experimentally, we have generated such a field by passing a semiconductor laser beam through a Michelson interferometer, thereby converting part of the intrinsic phase flucutations into amplitude fluctuations. We find indeed a shifted resonance frequency when this beam interacts with the Rb D_2 transition. Depending on the path-length difference of the interferometer, shifts of more than 10 MHz have been measured. The experiments have been performed in the weak-field limit. This allows a convolution-type interpretation of the stochastic realization shift.

I. INTRODUCTION

As pointed out by Camparo and Lambropoulos [1], the interaction of a two-level system with a quasimonochromatic field with a stochastically varying amplitude and phase is more complicated than the interaction with a truly monochromatic field (i.e., a field with a constant frequency and amplitude). Notably, the effective resonance frequency, defined as the frequency that maximizes the excitation of the two-level system, can be shifted with respect to that observed with a monochromatic field. This so-called stochastic realization shift occurs when the amplitude and phase fluctuations of the driving field are not independent, but correlated.

Amplitude-phase coupling intrinsically occurs in a semiconductor laser. This makes it natural, as pointed out by Camparo and Lambropoulos [1], to look for consequences of the stochastic realization shift in spectroscopy with semiconductor lasers. In a subsequent paper we have worked out this point [2]. We stressed a convolution-type interpretation of the stochastic realization shift: amplitude-phase coupling leads to asymmetry of the semiconductor laser spectrum and thus to a shift when this spectrum is convoluted with the symmetric absorption spectrum of a two-level atom. The asymmetry of the laser spectrum was shown to be most prominent at the relaxation oscillation sidebands, which occur at a few GHz [3,4].

Recently, it has been pointed out by Camparo and Klimcak that a convolution-type interpretation only applies in the weak-field limit [5]. This limit is defined as $\Omega_R \ll T_2^{-1}$, where Ω_R is the Rabbi frequency and T_2^{-1} is the dephasing rate of the atomic system. In the strong-field limit ($\Omega_R \gg T_2^{-1}$) the shift should be viewed as the consequence of an asymmetric dynamical response of the atoms due to amplitude-phase coupling of the stochastic fluctuations. Camparo and Klimcak provided experimental confirmation of a shift, using a microwave-driven hyperfine transition of rubidium (Rb). Both the weak-field and the strong-field regimes were investigated. However, in the experiment they did not use a stochasti-

cally varying field. In fact, they modulated the 6.8-GHz microwave field *sinusoidally*, in such a way that correlated harmonic variations of phase and amplitude were introduced. Unfortunately, the modulation frequency was chosen to be relatively large ($v_m = 271$ Hz), that is, even larger than the dephasing rate of the atomic system, estimated to be 120 Hz. At low power, a scan of the average microwave frequency over the atomic transition thus leads to an absorption spectrum in which the discrete sidebands of the microwave field are clearly resolved. At high power, broadening smears out the more or less discrete absorption spectrum to a continuum. This explains why, in the experiment of Camparo and Klimcak [5], the shift disappears in the low-field limit, while for a stochastically varying field the shift is expected to go to a constant, nonzero value in this limit.

In the present article we report an experimental demonstration of the resonance shift due to the correlation of the phase and amplitude fluctuations of a *stochastically* varying field interacting with an *optical* transition. We use a semiconductor laser which is tuned to the Rb D_2 transition near 780 nm. We do not use the intrinsic amplitude-phase coupling, which is relatively weak and present only on a short time scale [2]. Instead we introduce an artificial coupling by passing the beam of the semiconductor laser through a Michelson interferometer, with two arms of unequal length. The interferometer converts part of the natural phase variations of the input beam, which are induced by spontaneous emission and observable as the fundamental (Schawlow-Townes) laser linewidth, into amplitude fluctuations of the output beam [6,7]. Obviously, the amplitude and phase fluctuations of the output beam are correlated. In fact, this correlation has been recently used to suppress the small intrinsic amplitude fluctuations of a semiconductor laser beam [8].

II. HOW TO IMPOSE AMPLITUDE-PHASE CORRELATIONS

When phase-diffusing light, with constant amplitude E_0, is passed through a two-beam interferometer, the out-

put field is

$$E_{out}(t) = \tfrac{1}{2}E_0\cos\{2\pi\nu_l(t-t_1)+\phi(t-t_1)\}$$
$$+ \tfrac{1}{2}E_0\cos\{2\pi\nu_l(t-t_2)+\phi(t-t_2)\}$$
$$= E_0\cos\{\tfrac{1}{2}\Phi_0+\tfrac{1}{2}[\phi(t-t_1)-\phi(t-t_2)]\}$$
$$\times\cos\{2\pi\nu_l(t-t_{av})+\phi_{av}(t)\} , \quad (1a)$$

$$t_{av}=\tfrac{1}{2}(t_1+t_2) , \quad \phi_{av}(t)=\tfrac{1}{2}[\phi(t-t_1)+\phi(t-t_2)] , \quad (1b)$$

where t_1 and t_2 are the travel times through the two interferometer arms, ν_l is the laser frequency, $\phi(t)$ is the diffusing phase of the input field, and $\Phi_0=2\pi\nu_l(t_2-t_1)$ $(\mathrm{mod}2\pi)$ is the interferometer phase. Equation (1a) shows that stochastic variations of the phase of the input field lead to stochastic intensity variations in the output field and that the interferomter imposes an *amplitude*-phase correlation on the transmitted light. It is more convenient to work with the *intensity*-phase correlation, since this is more directly related to the optical spectrum, as can be seen from Fourier-type considerations. For phase-diffusing input light, we find

$$C_{I\phi}(t)\equiv\left\langle\left|\frac{(I_{out}(t'+t)+I_{out}(t'))}{2I_{in}}\right|\left|\frac{\phi(t'+t)-\phi(t')}{2\pi}\right|\right\rangle$$
$$= -\tfrac{1}{4}\sin(\Phi_0)\Delta\nu_l t e^{-\pi\Delta\nu_l t} \quad (0<t<\tau) , \quad (2)$$

where $\langle\ \rangle$ denotes (time) averaging over t'. I_{in} and I_{out} are the input and output power of the interferometer, $\Delta\nu_l$ is the [full width at half maximum (FWHM)] laser linewidth of the input light, and $\tau=t_2-t_1$ is the delay time of the interferometer. The normalized output power of the interferometer is

$$\left\langle\left|\frac{I_{out}(t'+t)+I_{out}(t')}{2I_{in}}\right|\right\rangle=\tfrac{1}{2}+\tfrac{1}{2}\cos(\Phi_0)e^{-\pi\Delta\nu_l|\tau|}$$
$$= \tfrac{1}{2}+\tfrac{1}{2}\cos(\Phi_0)\mathcal{V}(\tau) , \quad (3)$$

where we have introduced the fringe visibility $\mathcal{V}(\tau)$ for later use. Outside the range $(0<t<\tau)$ the intensity-phase correlation function $C_{I\phi}(t)$ has the following properties: (i) for $t>\tau$, $C_{I\phi}(t)=C_{I\phi}(\tau)$; and (ii) for $t<0$, $C_{I\phi}(t)=-C_{I\phi}(-t)$. Notice that when the interferometer phase is tuned from constructive ($\Phi_0=0$) to destructive interference ($\Phi_0=\pi$) the correlation between the phase fluctuations and intensity fluctuations first increases reaches a maximum at $\Phi_0=\pi/2$, and then decreases again. The latter decrease is mainly due to the reduction in output power [see Eq. (3)].

By calculating $\langle\Delta I_{out}^2\rangle$ one can show that at small delay and $\Phi_0=\pi/2$ (or $3\pi/2$) the relative strength of the induced intensity fluctuations is given by $\langle\Delta I_{out}^2\rangle/\langle I_{out}\rangle^2\approx\tau/\tau_{coh}$, where τ_{coh} is the coherence time of the input field. For laser light with spectral width (FWHM) $\Delta\nu_l$ we have $\tau_{coh}=1/(2\pi\Delta\nu_l)$. In our experiments we have typically $\tau/\tau_{coh}=0.0-0.6$ (see below). The induced amplitude-phase correlations are similar to the correlations that occur naturally in semiconductor lasers as a result of the dependence of the refractive index

on population inversion and that are usually described in terms of the linewidth enhancement factor α [9]. However, the induced fluctuations also occur at low frequencies (MHz), corresponding to the laser linewidth, whereas the intrinsic fluctuations, which are generally much smaller, are only relevant at high frequencies (GHz), corresponding to the carrier dynamics and relaxation oscillations. Therefore, the latter fluctuations will be neglected in this article.

III. EXPERIMENT

The semiconductor laser used in this experiment is an $Al_xGa_{1-x}As$ laser operating around 780 nm (Hitachi model HL7838G). The laser was carefully tuned to the Rb resonance line at 780 nm, by adjusting its temperature and current. It reached the relevant resonance at a temperature of approximately 12 °C and a current of 37.3 mA (threshold current 27.9 mA). The measured tuning coefficients are

$$\frac{\partial\nu}{\partial I}=-5.6\ \mathrm{GHz/mA} , \quad \frac{\partial\nu}{\partial T}\approx-30\ \mathrm{GHz/K} . \quad (4)$$

These derivatives clearly show that both the laser temperature and current have to be extremely stable to accurately measure a stochastic shift, expected to be of the order of a few MHz. The temperature was stabilized with a home-built double feedback loop based on a temperature-sensing resistor with a negative temperature coefficient (NTC) and two driving Peltier elements. From the error signal in the feedback loop one derives a temperature stability of about 50 μK (on a 1-min time scale). The laser current was supplied by a battery-driven Seastar LD2000 current supply with a specified current noise of 750 nA and a stability of 2 μA in 3–5 min. The current supply was found to be the prime source of frequency drift of the laser.

The Rb D_2 transition consists of four resolved components (Fig. 1), which represent the two isotopes ^{85}Rb (72%) and ^{87}Rb (28%) and the two ground-state hyperfine levels [10]. The excited-state hyperfine splitting (typically 100 MHz) is not resolved, due to the much larger Doppler width (520 MHz at $T=20$ °C). It does, however, lead to the spectral width of the four components being slightly larger than the Doppler width, namely 600 MHz. In the experiment we have concentrated on the transition starting from the $F=3$ ground state of ^{85}Rb to the $F'=2,3,4$ excited states (see dotted vertical line in Fig. 1). This transition is sufficiently isolated to be treated as a single line. To avoid optical pumping, the intensity of the optical beams used in the experiment is kept sufficiently low ($I<30\ \mu$W/cm^2) [11]. Effects of optical pumping were indeed observed for $I>100\ \mu$W/cm^2. The Rb cell had a peak absorption of about 40% over its 4-cm length.

To measure the expected shift of the resonance frequency, one has to determine that frequency within a fraction of a percent of the Doppler width. This requires a frequency modulation technique. For stability reasons we decided to keep the laser frequency fixed and modulate the transition frequency instead. For this purpose
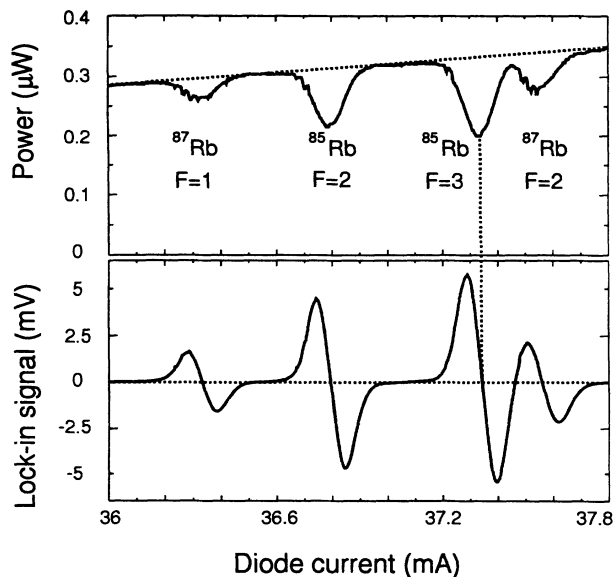
FIG. 1. Rb spectra obtained with the experimental setup of Fig. 2. The upper curve gives the optical power measured behind the Rb cell and the lower curve the lock-in signal as a function of the laser current (and thus the frequency). The Rb D_2 line consists of four resolved transitions, which originate from the $F=2$ and $F=3$ ground-state levels of ^{85}Rb and the $F=1$ and $F=2$ ground-state levels of ^{87}Rb. The dotted vertical line marks the transition that was used for the shift experiments.

the Rb cell was placed between two current coils, which generate a sinusoidally varying magnetic field. The magnetic field produces a splitting of the levels in magnetic sublevels, which shift by different amounts. The various $(\Delta m_F = +1)$ transitions, which can be excited with the circularly polarized beam (σ^+), will thus be shifted; this is the (anomalous) Zeeman effect. Below we will argue that, although the Rb line under investigation is composed of many $(\Delta m_F = +1)$ transitions, the modulating magnetic field will only lead to an effective modulation of the line center, and that broadening is negligible. The resulting power variations of the transmitted beam were recorded with a photodiode, connected to a lock-in amplifier. This makes the lock-in signal proportional to the *derivative* of the frequency-dependent optical transmission. The zero crossing of the lock-in signal corresponds to resonance. Close to this zero crossing the lock-in signal is proportional to the frequency detuning from resonance and can be used as a measure thereof.

A complication is the fact that the g_F factors of the $F=3$ ground-state hyperfine level and the $F'=2,3,4$ excited-state hyperfine levels differ $(g_{F=3}=\frac{1}{3}, g_{F'=2}=\frac{1}{9}, g_{F'=3}=\frac{7}{18}, \text{and } g_{F'=4}=\frac{1}{2})$, and that the various transitions thus shift by different amounts. This complication is hidden underneath the relatively large Doppler width, and the effective shift of the spectral line under investigation is simply the weighted average of the shifts of the individual components. One might think that the difference mentioned above will lead to an effective broadening of

the spectral line in a magnetic field. However, at least for small shifts, this effect is completely drowned by the much larger Doppler width. Experimentally, this is demonstrated by the fact that, upon scanning the average laser frequency the lock-in signal is (within 10%) proportional to the frequency derivative of the absorption profile (see Fig. 1).

The exact value of the ac magnetic field is not essential for the experiment. A rough estimate of 10 G (peak) was obtained with a Hall probe, after the Rb cell was removed. This is only a rough estimate, as the metallic clamp holding the Rb cell will almost certainly change the magnetic field. From the observed frequency modulation of 20-MHz peak zero, we estimate that the magnetic field with the Rb cell in place was probably about a factor of 3 larger.

Figure 2 shows the experimental setup. The laser beam is first passed through a 35-dB isolator (ISO) to optically isolate the laser diode from the setup, and then split in two. The *reference* beam passes through a neutral density filter (NDF), a $\lambda/4$ plate, and the Rb cell, before its intensity is detected with a photodiode. The *signal* beam first passes through an off-axis Michelson interferometer, which imposes a certain amount of amplitude-phase coupling. The signal beam then also passes through a NDF, a $\lambda/4$ plate, and the Rb cell, to be detected on a different photodiode. The path-length difference of the arms of the interferometer can be coarse adjusted by moving one of the corner cubes on an optical rail and fine adjusted with a piezoelectric element attached to the other corner cube. The signal and reference beam are parallel, but overlap nowhere. Their powers are adjusted with individual neutral density filters to be 0.3 μW in front of the Rb cell in a beam of 1.5-mm diameter. The two detecting photodiodes are connected to two different lock-ins which thus record the intensity variations of the transmitted signal and reference beam.

First the stability of the laser and the performance of the setup were checked. This was done by blocking one path of the interferometer, making the beams equally intense, tuning the laser frequency roughly to optimum absorption, that is to the zero crossing on the lock-ins and monitoring the signal as a function of time. The result is shown in Fig. 3. For clarity, both lock-in readings have been shifted downwards by different amounts. The measured variations are almost completely due to frequency drift of the laser; far off resonance, hardly any variations are observed. The lock-in readings can be easily converted into a frequency scale (see right-hand axis of Fig. 3) by using the measured sensitivity $\partial V_{\text{lock-in}}/\partial \nu_l = 50$ μV/MHz for calibration. The frequency drift of the laser is thus found to be at most 4 MHz in a second and 10 MHz in a minute, apparently determined by the stability of the current source. The upper curve in Fig. 3 was obtained by subtracting the two lock-in signals. The variations in this curve are quite small, showing that to first order the two beams and two detection systems behave identically. The rms voltage fluctuation in the difference signal is only 20 μV, indicating that a stochastic realization shift as small as 0.4 MHz should be observable.

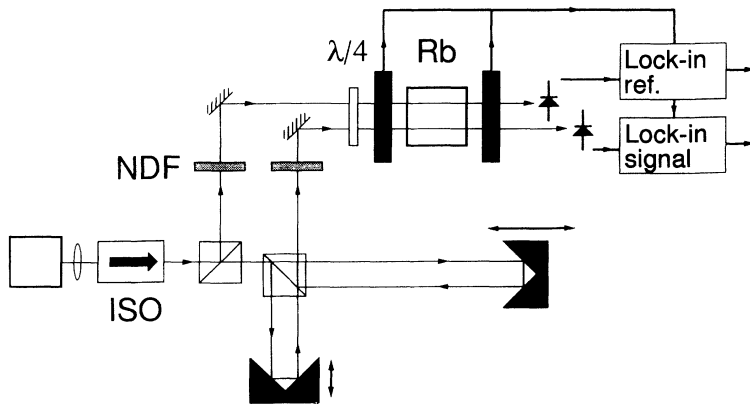In the actual experiment both arms of the interferome-

FIG. 2. Experimental setup. NDF denotes a neutral-density filter and ISO is an optical isolator.

ter contribute to the signal beam. At constructive interference and short delay this beam is made equally strong as the reference beam. The interferometer is coarse adjusted to a certain time delay $\tau = 2\Delta L/c$, where ΔL is the length difference between the two arms. This length difference is then scanned over a few wavelengths with a computer-controlled piezoelectric element. As a consequence, the optical power of the signal beam exiting the interferometer changes dramatically from constructive interference ($\Phi_0 = 0$) to destructive interference ($\Phi_0 = \pi$) and so on. During this scan, which took 1–2 min, we monitored the power of the signal beam and the readings of the two lock-ins. We experimentally deduced the interferometer phase Φ_0 from the measured power of the signal beam [see Eq. (3)], in order to be less susceptible to drift of the interferometer and hysteresis of the piezoelectric element.

The early experimental runs were troubled by a spurious signal due to mechanical vibrations in the corner cubes induced by the oscillating magnetic field across the Rb cell. The spurious signal was removed by vibrational isolation of the current coils and by magnetic shielding with a large tube of μ metal positioned around the

current coils and the Rb cell.

A scan of the interferometer phase leads to a change of power in the signal beam and thus, when the laser is (slightly) off resonance, to a change in lock-in reading even in the absence of a stochastic realization shift. To correct for this trivial power dependence, we multiply the reading of the reference lock-in, which simply registers the frequency drift of the semiconductor laser, with the ratio of the optical power in the signal and reference beam and subtract this result from the reading on the signal lock-in. The thus obtained corrected lock-in signal, which will be called $V_{\text{lock-in}}$ throughout the rest of the paper, is insensitive to frequency drift of the laser and should be zero in the absence of a stochastic realization shift.

Figure 4 shows the dependence of the corrected lock-in signal $V_{\text{lock-in}}$ on Φ_0 for three different delays: $\Delta L = -4$, 4, and 20 cm. The data are well fitted by functions of the form $C(\Delta L)\sin(\Phi_0)$, where the amplitude $C(\Delta L)$ is a
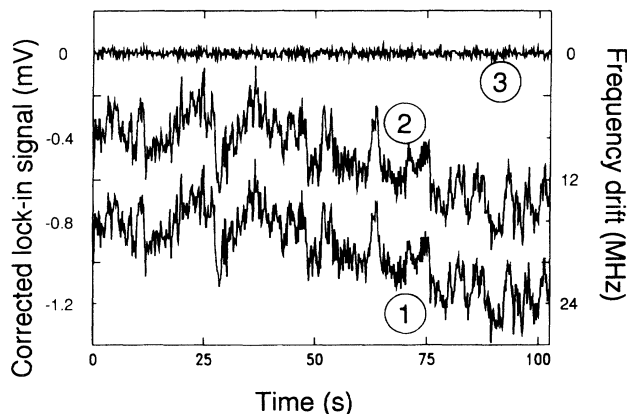

FIG. 3. Drift of the laser frequency as a function of time. Curve 1 shows the reading of the signal lock-in. Curve 2 shows the reading of the reference lock-in. Curve 3 denotes the difference between curves 1 and 2.
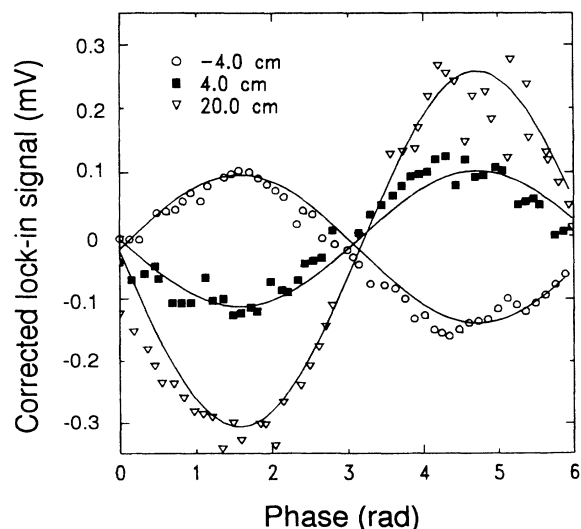

FIG. 4. The deviation from resonance, as measured with the signal lock-in and corrected for drift of the laser frequency, plotted as a function of the average interferometer phase Φ_0. This figure contains runs taken at three different delays: $\Delta L = -4, 4$, and 20 cm.
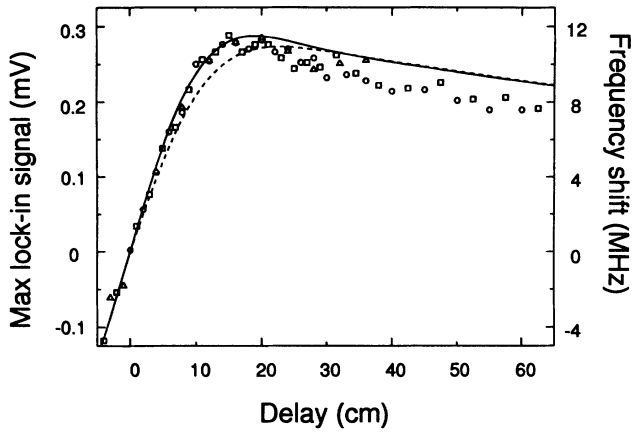
FIG. 5. The maximum corrected lock-in signal plotted as a function of delay ΔL. This signal is a measure for the stochastic realization shift.

measure for the predicted stochastic realization shift. $V_{\text{lock-in}}$ is largest midway on the slopes of the interferometer transmission curve ($\Phi_0 = \pi/2$ and $3\pi/2$), where phase fluctuations induce the largest intensity fluctuations.

Measurements of the shift have been performed at many different delays. Figure 5 summarizes these results in the dependence of the amplitude $C(\Delta L)$ on the delay ΔL. The main conclusions are as follows: (i) At zero delay there is no shift, (ii) a change from positive to negative delay leaves the magnitude of the shift intact but changes its sign, (iii) at small delays the shift increases linearly with delay, and (iv) the shift reaches a maximum at a delay of roughly 20 cm and slowly decreases at larger delay. At a delay of 20 cm the maximum corrected lock-in signal is $V_{\text{lock-in}} \approx 0.28$ mV at $\Phi_0 = \pi/2$. Combining this value with the sensitivity of 50 μV/MHz at full power, one might think that the shift is 5.6 MHz. However, at $\Phi_0 = \pi/2$ the power in the signal beam is only about half the power at constructive interference and one thus finds that the stochastic realization shift in this situation actually is about 11.2 MHz.

IV. THEORY

It is possible to directly calculate the stochastic realization shift from the intensity-phase correlation as given by Eq. (2), but the calculation is easier in the frequency domain. Since we consider the weak-field limit, the interaction of the optical beam with the atomic system is linear and it is possible to treat each frequency component separately and finally integrate over the spectrum of the driving field. The interferometer and the Rb cell are then considered as spectral filters with transmission functions $T_{\text{int}}(v)$ and $T(v-v_{\text{Rb}})$, respectively. The modulation of the Rb eigenfrequency v_{RB} induced by the magnetic field, results in a modulation of the transmitted intensity proportional to $\partial T(v-v_{\text{Rb}})/\partial v_{\text{Rb}}$ for each frequency component. Integration over the optical spectrum gives the overall intensity modulation and the (corrected) lock-in signal $V_{\text{lock-in}}$,

$$V_{\text{lock-in}} \propto -\int_0^\infty dv \left[\frac{\partial T(v-v_{\text{Rb}})}{\partial v_{\text{Rb}}}\right] T_{\text{int}}(v)L(v-v_l) ,$$

(5a)

$$T(v-v_{\text{Rb}}) = \exp\left[-A\exp\left\{-4\ln2\frac{(v-v_{\text{Rb}})^2}{\Delta v_{\text{Rb}}^2}\right\}\right] ,$$

(5b)

$$\frac{\partial T(v-v_{\text{Rb}})}{\partial v_{\text{Rb}}} = -8\ln2\frac{(v-v_{\text{Rb}})}{\Delta v_{\text{Rb}}^2}$$

$$\times \exp\left\{-4\ln2\frac{(v-v_{\text{Rb}})^2}{\Delta v_{\text{Rb}}^2}\right\}AT(v-v_{\text{Rb}}) ,$$

(5c)

$$T_{\text{int}}(v) = \tfrac{1}{2} + \tfrac{1}{2}\cos\{\Phi_0 + 2\pi\tau(v-v_l)\} ,$$

(5d)

$$L(v-v_l) = \left[\frac{\Delta v_l}{2\pi}\right]\frac{1}{(v-v_l)^2 + (\Delta v_l/2)^2} ,$$

(5e)

where $A = -\ln[T(v=v_{\text{Rb}})]$ and Δv_{Rb} are the depth and (FWHM) spectral width of the Rb absorption and $L(v-v_l)$ is the normalized Lorentzian spectrum of the input laser light.

One can calculate $V_{\text{lock-in}}$ by substituting the appropriate expressions underneath the integral of Eq. (5a) setting ($v_l = v_{\text{Rb}}$) and comparing the result with the sensitivity $\partial V_{\text{lock-in}}/\partial v_l$ measured without interferometer [$T_{\text{int}}(v) \equiv 1$]. The integral can be solved by expanding the factor $T(v-v_{\text{Rb}})$, which appears underneath the integral when (5c) is substituted into (5a), in powers of $\exp[-4\ln(2)(v-v_{\text{Rb}})^2/\Delta v_{\text{Rb}}^2]$ and evaluating each term separately. When $\Delta v_{\text{Rb}} \gg \Delta v_l$, the factor $T(v-v_{\text{Rb}})$ is approximately constant over the relevant frequency range and the first term in the expansion dominates. One then finds

$$V_{\text{lock-in}} \approx -\tfrac{1}{8}\sin(\Phi_0)\frac{\partial V_{\text{lock-in}}}{\partial v}\Delta v_l$$

$$\times \left\{e^{\pi\Delta v_l\tau}\left[1-\text{erf}\left[\frac{\pi\Delta v_{\text{Rb}}\tau}{2\sqrt{\ln2}}\right]\right]\right.$$

$$\left. + e^{-\pi\Delta v_l\tau}\left[1+\text{erf}\left[\frac{\pi\Delta v_{\text{Rb}}\tau}{2\sqrt{\ln2}}\right]\right]\right\} ,$$

(6)

where erf is the error function. In Fig. 5 two theoretical fits are shown: the dashed curve is based on Eq. (6), whereas the solid curve also includes contributions due to higher-order terms in the expression discussed above. For both fits we used a laser linewidth of $\Delta v_l = 26$ MHz and an absorption Doppler width of $\Delta v_{\text{Rb}} = 600$ MHz. In a separate experiment we determined Δv_l by measuring the fringe visibility $\mathcal{V}(\tau)$ using the same Michelson interferometer [see Eq. (3)]. The result of that experiment ($\Delta v_l = 25$ MHz) was in very good agreement with the value used for the fit of Fig. 5.

The results in Fig. 5 can be understood in terms of spectral filtering. Three frequency widths are important: the laser linewidth Δv_l, the absorption width Δv_{Rb}, and the frequency separation of the interferometer fringes

$\Delta v_{\mathrm{FSR}} \equiv 1/(2\pi\tau)$, where FSR stands for free spectral range. Equation (6) has been derived under the assumption that $\Delta v_l \ll \Delta v_{\mathrm{Rb}}$. We can now distinguish between two situations. At small delay $(\Delta v_{\mathrm{FSR}} > \Delta v_{\mathrm{Rb}})$ the spectral filtering due to the interferometer occurs mainly at frequencies beyond the atomic absorption line. This filtering is therefore hardly effective and the measured frequency shift will be relatively small; in fact, it increases linearly with delay time τ. At large delay $(\Delta v_{\mathrm{FSR}} < \Delta v_{\mathrm{RB}})$ the spectral filtering occurs dominantly underneath the absorption line. The shift is then almost independent of delay and decreases slowly, only due to the loss of coherence between light from the two arms of the interferometer. In this limit, which is experimentally reached for $\Delta L > 20$ cm, the stochastic realization shift is a property of the output beam of the interferometer that is independent of the atomic system (i.e., of Δv_{Rb}) and is solely related to the amplitude-phase coupling of the stochastic field.

For a very broad absorption line, which senses practically all spectral deformation produced by filtering in the interferometer, we are practically always in the limit $(\Delta v_{\mathrm{Rb}} \gg \Delta v_{\mathrm{FSR}})$ so that (at $v_l = v_{\mathrm{Rb}}$)

$$\frac{\partial T(v - v_{\mathrm{Rb}})}{\partial v_{\mathrm{Rb}}} \propto -(v - v_{\mathrm{Rb}}) , \tag{7a}$$

$$V_{\text{lock-in}} \propto \int_0^\infty dv(v - v_l) T_{\mathrm{int}}(v) L(v - v_l) , \tag{7b}$$

$$v_{\mathrm{shift}} = \frac{\int_0^\infty dv(v - v_l) T_{\mathrm{int}}(v) L(v - v_l)}{\int_0^\infty dv\, T_{\mathrm{int}}(v) L(v - v_l)} , \tag{7c}$$

where the denominator in Eq. (7c) is introduced to normalize the spectrum of the light exiting the interferometer. One then finds

$$V_{\text{lock-in}} = -\tfrac{1}{4}\Delta v_l \frac{\partial V_{\text{lock-in}}}{\partial v} \sin(\Phi_0) e^{-\pi\Delta v_l \tau} , \tag{8a}$$

$$\Delta v_{\mathrm{shift}} = -\tfrac{1}{2}\Delta v_l \frac{\sin(\Phi_0) e^{-\pi\Delta v_l \tau}}{1 + \cos(\Phi_0) e^{-\pi\Delta v_l \tau}} . \tag{8b}$$

These equations show that the maximum corrected lock-in signal is observed at $\Phi_0 = \pi/2$ and $3\pi/2$. For a very broad absorption line the shift is then exactly half the laser linewidth. Larger shifts occur closer to destructive interference $(\Phi_0 \approx \pi)$, mainly because the denominator in Eq. 8(b) (equal to optical power) becomes small. For small delay, the spectrum is then strongly deformed and shifts of many times the laser linewidth Δv_l are possible. However, the spectral deformation stretches out to large frequencies and is only observable with an extremely broad absorption line.

V. DISCUSSION AND CONCLUSIONS

One might say that the occurrence of the stochastic realization shift in the weak-field limit results from the ambiguity of the concept "the average frequency of the stochastic field." One definition of the average frequency is based on "a count of the optical cycles." If the sto-

chastically varying field would be beaten against a monochromatic field with frequency v_{LO} (as local oscillator), a simple count of the beat frequency would give $v_l - v_{\mathrm{LO}}$. Using this definition it seems that passage through an interferometer does not change the average frequency, because optical cycles do not get lost. Alternatively, one can define the average frequency as the average instantaneous frequency, but weighted with the (instantaneous) intensity of the stochastic field. If, due to amplitude-phase coupling, the intensity is, e.g., preferentially large when the instantaneous frequency is large, this weighted average will give a value (slightly) larger than v_l. The optical spectrum will then be asymmetric and its center of gravity will be shifted to a frequency slightly larger than v_l.

Via Fourier transformation it is possible to derive the following important equation, which is valid for any (stochastically varying) field:

$$\Delta v_{\mathrm{shift}} = \frac{\langle I(t)\dot{\phi}(t)/2\pi\rangle}{\langle I(t)\rangle} = \int_0^\infty dv(v - v_l) S(v) , \tag{9}$$

where $S(v)$ denotes the normalized spectrum of the driving field. Equation (9) shows that the definition of the average frequency as a weighted average of the instantaneous frequency always coincides with the center of gravity of the spectrum. A difference between this "average frequency" and the one obtained from a count of optical cycles (v_l) can lead to a stochastic realization shift.

It is interesting to note that the stochastic realization shift is related to the so-called "Wolf shift." In Ref. [13] Wolf showed that the optical spectrum emitted by an extended source which exhibits spectral correlations between different spatial regions is in general not invariant under propagation. As an example, he calculated how the combined spectrum emitted by two small spatially separated sources depends on their correlation [14]. The resulting Wolf shift has been first experimentally demonstrated for two acoustic sources driven by correlated noise [15]. It was also later demonstrated for two correlated optical sources, created by joint illumination of two slits with light from the two spectrally filtered halogen lamps [16]. In our experiment, the optical beams emitted from the two arms of the interferometer can also be interpreted as spectrally correlated sources, the separation now being in the time domain instead of the space domain. Our use of an interferometer results in a field whose intensity-weighted average frequency is a kind of time analog of the Wolf shift. Note, however, that in general the intensity-weighted average frequency is not the same thing as the stochastic realization shift; this is only true in the weak-field limit. In strong fields, where nonlinear effects become important, the stochastic realization shift is a more complicated quantity [17].

We have shown that the optical resonance as observed with a nonmonochromatic driving field can be shifted when this field has correlated amplitude and phase fluctuations. In practice, this correlation will quite naturally occur when light is transported through an optical fiber with uncoated (and thus reflecting) facets. The magnitude of the shift is typically a fraction of the spectral width of the driving field and is thus mainly important

for high-precision experiments. It may play a role in experiments where semiconductor lasers are optically and/or electronically locked onto an optical transition to create a frequency standard [12].

In the weak-field limit, the stochastic realization shift is basically a result of spectral filtering. At large intensity, when the spectral absorption becomes power broadened, the convolution-type interpretation given in this article becomes invalid, as the system's response becomes nonlinear. The effective resonance frequency will then also depend on higher-order correlation function of the amplitude and phase of the stochastically varying driving field. Since the case of linear filtering as discussed in this article is already quite complicated, this will apply even more to the case of nonlinear filtering [1,5].

ACKNOWLEDGMENTS

[1] J. C. Camparo and P. Lambropoulos, Opt. Commun. 85, 213 (1991).

[2] M. P. van Exter and J. P. Woerdman, Opt. Commun. 88, 336 (1992).

[3] K. Vahala, Ch. Harder, and A. Yariv, Appl. Phys. Lett. 42, 211 (1983).

[4] M. P. van Exter, W. A. Hamel, J. P. Woerdman, and B. R. P. Zeijlmans, IEEE J. Quantum Electron. QE-28, 470 (1992).

[5] J. C. Camparo and C. M. Klimcak, Opt. Commun. 91, 3443 (1992).

[6] J. A. Armstrong, J. Opt. Soc. Am. 56, 1024 (1966).

[7] R. Centeno Neelen, D. M. Boersma, M. P. van Exter, G. Nienhuis, and J. P. Woerdman, Phys. Rev. Lett. 69, 593 (1992).

[8] M. A. Newkirk and K. J. Vahala, IEEE J. Quantum Electron. QE-27, 13 (1991).

[9] C. H. Henry, IEEE J. Quantum Electron. QE-18, 259 (1982).

[10] J. R. Beacham and K. L. Andrew, J. Opt. Soc. Am. 61, 231 (1977).

[11] A. M. Akulshin, V. A. Sautenkov, V. L. Velichansky, A. S. Zibrov, and M. V. Zverkov, Opt. Commun. 77, 295 (1990).

[12] M. Têtu, B. Villeneuve, N. Cyr, P. Tremblay, S. Thériault, and M. Breton, J. Lightwave Technol. 7, 1540 (1989).

[13] E. Wolf, Phys. Rev. Lett. 56, 1370 (1986).

[14] E. Wolf, Phys. Rev. Lett. 58, 2646 (1987).

[15] M. F. Bocko, D. H. Douglass, and R. S. Knox, Phys. Rev. Lett. 58, 2649 (1987).

[16] F. Gori, G. Guattari, C. Palma, and C. Padovani, Opt. Commun. 67, 1 (1988).

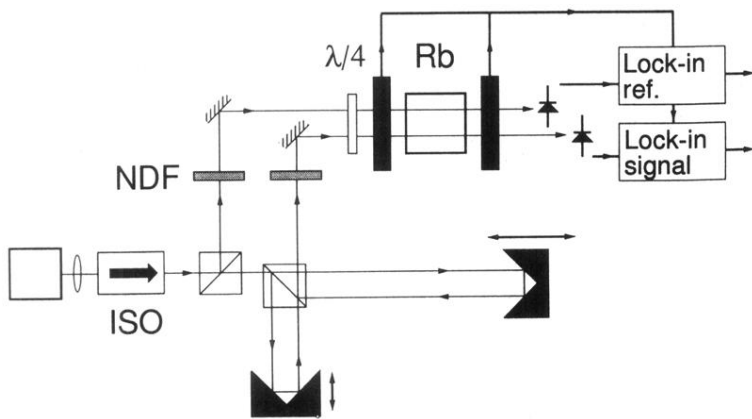[17] J. C. Camparo and P. P. Lambropoulos, J. Opt. Soc. Am. B 9, 2163 (1992)

FIG. 2. Experimental setup. NDF denotes a neutral-density filter and ISO is an optical isolator.